

State-of-the-art Report

Recent trends in monitoring tunnelling-induced displacements of structures

Tendances récentes en matière de surveillance des déplacements induits par le creusement des tunnels sur les structures

E. Bilotta*

University of Napoli Federico II, Naples, Italy

**emilio.bilotta@unina.it*

ABSTRACT: Monitoring and control of tunnelling induced displacements in urban areas are a matter of primary importance to minimise excavation risks and enhance project acceptance. For this purpose, suitable and reliable monitoring techniques are routinely adopted in underground construction. Fast progresses in sensor technology have boosted the development of innovative monitoring for tunnel projects through prototypes and field trials. The latter have been generally carried out in conjunction with the routine conventional monitoring, allowing for comparison and validation. Consequently, a wide interest has been generated around some innovative techniques that permit real-time control of induced strain of structures (e.g. fibre optics), allow for historical movements trends (e.g. InSAR), and may provide cost-effective additional information (e.g. LiDAR and photogrammetry). At the same time, resolution, power supply and communication potential of conventional measuring techniques for displacement monitoring have largely improved in recent years. This paper reviews the state-of-art of monitoring the displacements induced by tunnel construction and explores the current trends in developments of innovative sensing techniques.

RÉSUMÉ: La surveillance et le contrôle des déplacements induits par le creusement des tunnels dans les zones urbaines sont d'une importance primordiale pour minimiser les risques liés à l'excavation et améliorer l'acceptation du projet. À cette fin, des techniques de surveillance appropriées et fiables sont régulièrement adoptées dans les constructions souterraines. Les progrès rapides de la technologie des capteurs ont stimulé le développement d'une surveillance innovante pour les projets de tunnels à travers des prototypes et des essais sur le terrain. Ces derniers ont généralement été associés à la surveillance conventionnelle de routine, ce qui a permis de les comparer et de les valider. Par conséquent, un grand intérêt a été suscité par certaines techniques innovantes qui permettent un contrôle en temps réel de la déformation induite des structures (par exemple, la fibre optique), permettent de suivre les tendances historiques des mouvements (par exemple, l'InSAR), et peuvent fournir des informations supplémentaires rentables (par exemple, LiDAR et photogrammétrie). Dans le même temps, la résolution, l'alimentation électrique et le potentiel de communication des techniques de mesure conventionnelles pour la surveillance des déplacements se sont largement améliorés ces dernières années. Cet article passe en revue l'état de l'art en matière de surveillance des déplacements induits par la construction de tunnels et explore les tendances actuelles en matière de développement des techniques de surveillance innovantes.

Keywords: Tunnelling; monitoring; structures; displacements; innovation.

1 INTRODUCTION

Tunnel construction in the built environment requires careful control of induced displacements through suitable and reliable monitoring techniques (Mair, 2008). In the last decade, innovative monitoring systems have attracted wide interest and they have been progressively applied in tunnel projects in addition to conventional sensing. Nonetheless, conventional monitoring techniques have been not discontinued and their resolution, power supply and communication

potential have largely improved in recent years (Ma et al., 2021). Nowadays monitoring tunnel construction provides a large volume of data to be processed, to alert of potential risk and trigger immediate corrective actions (Meyer et al., 2013; Gonzalez-Arteaga et al., 2020). Further, gathered data can feed existing digital twins of the construction process (Boje et al., 2020; Pan and Zhang, 2021), thus expanding the potential use of sensing techniques to “performance monitoring” in the whole tunnel life-cycle (Soga et al., 2019).

Starting from the state-of-art of techniques for monitoring displacements induced by tunnel construction on adjacent buildings, this paper explores the current trends in the development of innovative sensing technologies, focusing on the results of pilot applications that have proven their reliability and potential to enhance the whole structures' life-cycle.

2 MONITORING IN TUNNEL PROJECTS

In tunnel engineering, displacements need to be measured inside the tunnel cavity, for safety reasons and to ensure that the tunnel deformation falls within prescribed limits that guarantee its stability in both the short- and the long-term (e.g. convergence, extrusion, lining deflection), as well as above the tunnel to control induced ground and building movements (Figure 1). Deformation of the lining structures and tilt of buildings also require to be measured. The emphasis of structural health monitoring in tunnelling has traditionally been put on displacements (Brownjohn, 2007), and more recently on strain.

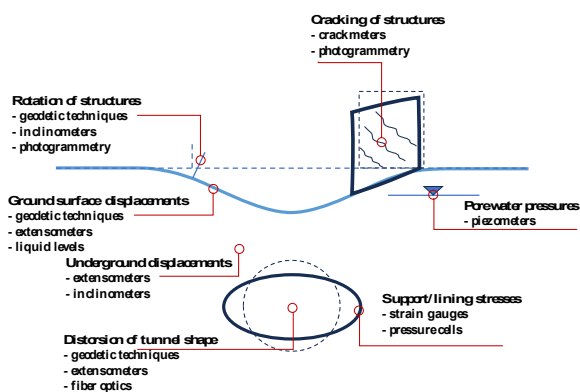


Figure 1. Tunnel construction and associated monitoring (modified from Hoult and Soga, 2014).

An overview of currently adopted measurement techniques for displacement, rotation and strain is shown in Table 1, with an indication of their range, resolution, and accuracy (BTS/ICE, 2004; ITA-AITES, 2011; Hoult and Soga, 2014; Morino et al., 2023).

Digital optical levelling is routinely performed to measure with high accuracy vertical movements on staffs and pins. *Laser distance meters* are also used for automatic and continuous measurement of convergence of the tunnel section, with accuracy up to ± 0.5 mm. *Total stations* (either manually or automatically operated) are primarily used to measure tunnel lining inflection and tunnelling-induced building deformation with an accuracy of ± 1 mm, or ± 2 mm if reflector-less (Hoult and Soga, 2014).

Laser scanner technology is also widely used in tunnelling since it enables a distributed assessment of

convergence and deformation of the tunnel cavity as well as displacements of aboveground structures. Compared to point measurements, such as those operated by total stations, laser scanners can detect up to 2 million points per second, thus generating large point cloud data sets (cf. § 3.3). Light-Detection-And-Ranging (*LiDAR*) technology, adopted by high-resolution terrestrial laser scanners, is suitable to detect movements inside the tunnel with good accuracy (about ± 1.5 mm) since it does not require external lighting and it is robust in wet environments containing air particulate. Using the latest technology and in the most favorable conditions displacements may be detected with an accuracy up to ± 0.5 mm (Walton et al., 2018).

Global Navigation Satellite Systems (GNSS), providing signals from space that transmit positioning and timing data to receivers on Earth, allow the height of a point above sea level (orthometric height) to be measured with an accuracy of 10 mm without conventional levelling (Meyer et al., 2005). Hence, they are suitable for monitoring “visible” building displacements (i.e. along the line of sight to at least five orbiting GNSS satellites). Currently, by installing a network of high-frequency receiving antennas and adopting the best-performing Real-Time Kinematic (RTK) positioning technique (Odolinski and Teunissen, 2020), an accuracy of about ± 1 mm may be achieved on quasi-static structural displacements, compared to Precise Point Positioning technique (PPP, Zumberge et al., 1997), that reaches about ± 5 mm (Qu et al., 2022).

Satellite constellations equipped with SAR, Synthetic Aperture Radars, permit radar images of the Earth surface to be acquired, providing information on the distance between the radar and the reflecting point (Cumming and Wong, 2005). Interferometric analysis of phase differences between two images (InSAR) allows the ground elevation to be measured with high accuracy (Digital Elevation Model, DEM), while movements of points on the ground surface can be detected by Differential Interferometry (DInSAR), as it will be discussed in § 3.2. For instance, the *Persistent Scatterer SAR Interferometry* (PS-InSAR) is suitable for measuring deformations in urban areas and its use to detect displacements induced by tunnelling on buildings has increased recently, achieving millimetric accuracy. Terrestrial applications of SAR interferometry have been also developed, where the antennas move on a track in front of the object, rather than along the satellite orbit.

Table 1 also provides information on the accuracy of *hydrostatic levelling systems* for measuring vertical displacements through pressure head changes with respect to a reference tank, of *inclinometers*, using

biaxial servo-accelerometers or MEMS for monitoring horizontal ground displacements at depth, through *inclinometers*, and *borehole extensometers* for monitoring displacements in the ground. Structural tilt is measured by means of electrolevels, servo-accelerometer or MEMS sensors (*tiltmeters*).

Changes of crack width in structures undergoing movements are locally monitored by installing on their surface *wire extensometers* or *crackmeters* (for smaller measurement base). *Photogrammetry* is increasingly being used for crack detection (Stent et al., 2016), as discussed in § 3.3.

Monitoring structural strain is very important to control the performance of both the supporting tunnel lining and the tunnelling-affected nearby structures and buildings, either directly or through stresses that can be derived. Although structural strains can be computed from measured displacements, it is common to measure them directly, by using dedicated sensors. The most used are *electrical strain gauges*, either measuring change of electrical resistance due to strain (*resistive type*) or measuring change of vibration frequency of a metallic wire upon stretching (*vibrating wire type*). The latter are widely used in tunnel monitoring since they are cheap, high reliable and durable (Morino et al., 2023). Alternatively, *fibre optic strain gauges* have been increasingly used in the last decades (Moss and Matthews, 1995; Soga and Schooling, 2016; Floris et al., 2021), and they are becoming more common in tunnelling, as discussed in § 3.1.

Table 1. Features of monitoring techniques/sensors.

| | device | range | resolution | accuracy |
|---------------------------|---------------------------|------------------------|------------------|--|
| displacement and rotation | Digital optical levels | distance up to 30 m | 0.1 - 0.01 mm | ± 0.3 mm/km |
| | Laser distance meters | distance up to 150 m | 0.1 mm | up to ± 0.5 mm |
| | Total stations | distance up to 1 km | 0.1 mm | up to ± (0.6 mm + 10 ⁻⁶ × dist. in mm) up to ± 0.1 mm diff disp. |
| | Laser scanner | distance up to 30 m | variable | up to ± 1.5 mm up to ± 8 arcseconds |
| | GPS/GNSS | distance up to 15 km | variable | ± 5 mm in plan ± 10 mm in height |
| | PS-InSAR | any | variable | ± 1 mm/year |
| | Hydrostatic levelling | up to 100 mm | 0.01 mm | up to ± 0.1 mm |
| | Inclinometer | ± 53° from vertical | 0.04 mm/m | ± 0.2 mm/m |
| | Tiltmeter | 50 to 175 mm/m | 0.05 to 0.3 mm/m | ± 0.1 mm/m |
| | Wire extensometer | meters | 0.01 mm | ± 1 mm |
| | Crackmeter | up to 150 mm | 0.01 mm | up to ± 0.01 mm |
| Borehole extensometer | up to 200 mm | up to 0.01 mm | up to ± 0.1 mm | |
| strain | Electrical strain gauges | vib. wires: up to 0.3% | 0.5 to 1 µε | vibrating wires: up to ± 1 µε |
| | Fibre-optic strain gauges | up to 1% | up to 1 µε | up to ± 10 µε |

3 EMERGING TECHNOLOGIES

Most of the well-established “conventional” geodetic techniques to monitor tunnelling induced displacements, namely digital optical levels and automatic total stations, share the common feature to achieve accurate measurements with relatively few data collection and processing. On the other hand, these measurements are spatially discontinuous. For this reason, in some cases critical mechanisms can be hard to reveal. Emerging techniques, such as laser scan or photogrammetry, and at a larger scale SAR differential interferometry, provide clouds of point measurements, that may be processed to obtain distributed information about change of surface conditions, hence continuous displacement profiles and deformation patterns. Fibre-optic sensing also results in distributed or quasi-distributed strain measurements over long distances. All these “emerging” techniques produce data of high resolution and large spatial coverage at relatively low cost at the field scale. Over the past decade, they have undergone significant validation in pilot applications that hint at a step change in tunnelling-induced displacement and strain monitoring.

3.1 Fibre-optics sensors

An optical fibre is a cylindrical structure that transmits light along its axis and is essentially made of three coaxial parts (Figure 2): a photosensitive core that carries the light, usually made of pure silicon dioxide (SiO₂) glass, a surrounding cladding made of glass with a lower refractive index (by means of a different level of impurities), a buffer coating outside, made of acrylate or polyamide, that protects the brittle fibre. Due to the core higher refractive index (RI), compared to the cladding, the light travelling in the core is reflected at the core-cladding interface. Single- or multi-mode fibres differ each other for the number of potential paths that light can take, depending on the size and refracting index variation in the core. Since propagation at higher modes decreases the signal-to-noise ratio (Nöther, 2010), single-mode fibres are generally preferred for long distances. In addition to glass fibres, polymer optical fibres (POFs) are also available, where the core is commonly made with polymethyl methacrylate (acrylic glass). However, POFs have very high attenuation compared to silica, which results in very low transmission distances.

Optical reflectometry techniques are useful to characterize optical fibres, in the time (Optical Time Domain Reflectometry, OTDR), coherence (Optical Coherence Domain Reflectometry, OCDR) and frequency domain (Optical Frequency Domain Reflectometry, OFDR).

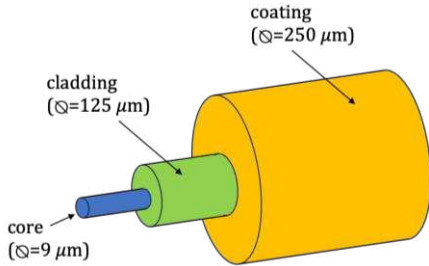


Figure 2. Structure of a single-mode optical fibre.

By using a visible laser propagating along the fibre core, Hill et al. (1978) created a periodic structure (grating) in the core with an increased refractive index, which generates a wavelength-specific dielectric Bragg mirror. The possibility to scan over the signals returned by the gratings kick-started the use of communication optical fibres as testing sensors to

measure strain or temperature that, affecting their central wavelength, modify their ability to reflect and transmit light. Meltz et al. (1989) engraved the first Fibre Bragg Grating (FBG) sensor in the core of a germanosilicate optical fibre exposed to an interference pattern of ultraviolet laser light with a specific wavelength (Figure 3a). Since then, several different techniques were developed to permit the multiplexing of many FBG sensors along a single fibre (Davis and Kersey, 1997), hence their use in many structural sensing applications. Optical frequency domain reflectometry (OFDR) can nowadays be used to measure the wavelength of light reflected from thousands of low reflectivity Bragg gratings, distributed along single-mode fibres (Childers et al., 2001), allowing for quasi-distributed FBG (DFBG) technology (Vlachopoulos, 2023).

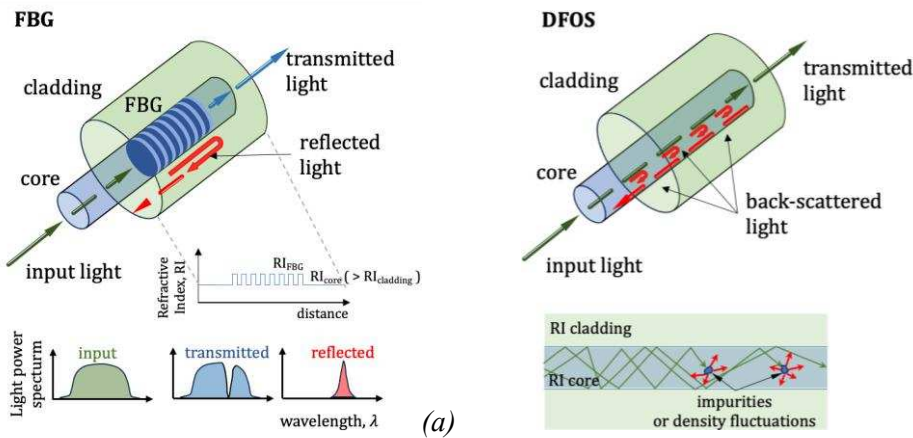


Figure 3. (a) FBG structure; (b) backscattered light along an optical fibre (modified after Kechavarzi et al., 2016 and Chai et al., 2019).

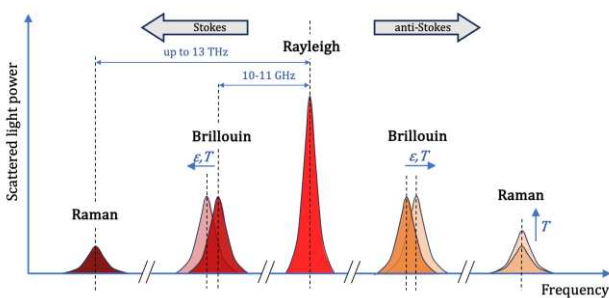


Figure 4. Backscattered light power spectra. ϵ , strain; T , temperature (modified from Kechavarzi et al., 2016).

Optical Backscatter Reflectometer (OBR), based on OFDR, uses light backscatter caused by random fluctuations in the refractive index profile along the fibre for the same purposes (Güemes et al., 2010). In fact, such perturbations, caused by the interaction of photons with impurities or density fluctuation within the fibre's core, behave like weak natural gratings engraved all along the fibre length (Figure 3b). Three types of light scattering exist: the linear Rayleigh

scattering, where the backscattered light has the same frequency as the transmitted light; the non-linear Brillouin scattering, that produces a shift in frequency of the backscattered light; the Raman scattering, that produces new photons with lower (Stokes-component) or higher (Anti-Stokes component) energy (Figure 4). Distributed fibre optic sensing technique (DFOS) takes advantage of the influence of strain and temperature change on the fibre refractive index, hence on the properties of the backscattered light.

The Rayleigh backscatter undergoes a shift in the local spectral frequency and a time shift, produced by the cumulative changes in the refractive index. Such spectral and temporal shifts can be measured by performing a cross-correlation on the backscattered light signals in the time-domain (OTDR) or in the frequency-domain (OFDR), and scaled to return distributed temperature or strain measurements (Güemes et al., 2010).

The frequency of the Brillouin peak, ν_b , is directly proportional to the acoustic velocity and refractive index and it shifts linearly with changes in longitudinal

strain and temperature in the fibre core (Soga, 2014; Kechavarzi et al. 2016):

$$\Delta v_b = C_\varepsilon \cdot \Delta\varepsilon + C_T \cdot \Delta T \quad (1)$$

C_ε and C_T slightly vary around values of 500 MHz/% and 1 MHz/°C, respectively, for standard telecommunication single mode fibres and at the operating wavelength of 1550 nm as used with Brillouin OTDR. Their value can be obtained by accurate calibration. Since the distance where the scattered light is generated can be calculated from the time interval between the launch of the pulsed light and the arrival of the backscattered light, once the fibre refractive index is known, the distribution of strain along the fibre can be obtained.

Another sensing method called Brillouin Optical Time Domain Analysis (BOTDA) can be used, that generally achieve larger accuracy. However, since it requires analysing the power difference between a pulse (pump) light and a continuous (probe) light sent in opposite direction from the two ends of the fibre, to stimulate the Brillouin scattering, it is unsuitable in case of fibre breakage during installation and monitoring (Soga and Luo, 2018).

For both FBG and DFOS the characteristics of FO measurements depend on the analyser (Table 2).

Table 2. Typical features of FO analysers (Vlachopoulos, 2023).

| technique | FBG | DFBG | BOTDR/ BOTDA | Rayleigh OFDR |
|----------------------------------|-------------------------|-------------------------|---------------------|---------------------|
| max sensing length | > 1000 m | < 50 m | > 1000 m | < 40 m |
| repeatability | ± 0.1-10 µε | ± 1 µε | ± 1 µε | ± 5 µε |
| spatial resolution | 0.10 m | ~ 6 mm | 0.1-1 m | 0.65 mm |
| max number of measurement points | 10-20 | > 1000 | > 1000 | > 1000 |
| sensing range | ± 17500 µε | ± 30000 µε | ± 30000 µε | ± 30000 µε |
| acquisition frequency | < 1000 Hz | < 250 Hz | < 1 Hz | < 60 Hz |
| unit price (approx. EUR) | 15k-120k | > 60k | 90k-250k | 50k-150k |
| sensor price (approx. EUR) | ~ 250 – 1000 per sensor | ~ 250 – 5000 per sensor | 0.10 per m of fibre | 0.10 per m of fibre |

An application of FBG to monitor the displacements induced to two heritage buildings by the excavation of a new tunnel for Bank Station Capacity Upgrade (BSCU) is described by Acikgoz et al. (2021, 2022).

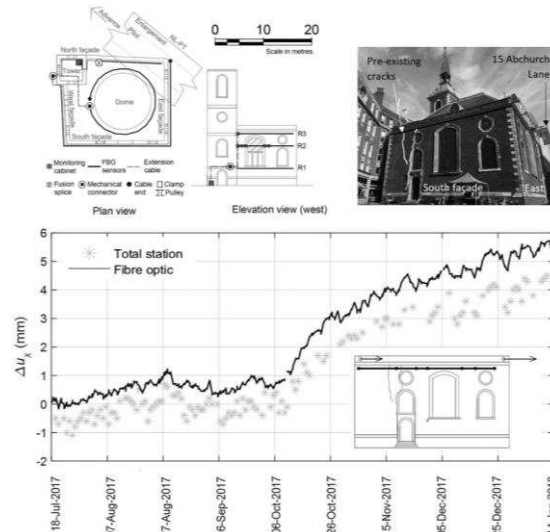


Figure 5. Monitoring St Mary Abchurch during BSCU: validation of FBG measurements against total station (modified after Acikgoz et al., 2021, 2022).

Figure 5 summarises the instrumentation installed on the masonry façades and dome of St. Mary Abchurch, including levelling targets, prisms and FBG optical fibres. The strains measured by FBGs deployed along the South façade of the church were integrated to obtain the relative horizontal displacements between the top corners of the façade, to be compared with displacements measured by a total station on a series of prisms. The time series plotted in Figure 5 along a period of about 6 months, corresponding to the pilot tunnel excavation and the enlargement, show the same trends in both datasets. The observed 1 to 2 mm differences were explained by the different locations of the prisms and fibre-optic sensors. Since the FBG data were validated by conventional measurements, fibre optic monitoring was continued after construction to measure the long-term effects on the church. Strain measurements confirmed that the consolidation-induced movements generally had a negligible effect on most of the structure. However, they produced an unexpected increase of the major pre-existing cracks in the South façade. This justifies careful crack detection and long-term monitoring of heritage buildings adjacent to tunnel excavation.

Kechavarzi et al. (2016) describe three case studies of pilot application of DFOS to monitor the deformation of existing tunnels due to adjacent tunnelling: an old-brick tunnel at the Thameslink King’s Cross station in London (Mohamad et al., 2010), a cast-iron Royal Mail tunnel at the Liverpool Street Crossrail station in London (Gue et al., 2015), and a segmental bolted tunnel lining of the Singapore MRT Circle Line 3 (Mohamad et al., 2012). In the earliest case, dating back to 2005, in addition to conventional monitoring of displacements induced by

the underpassing new tunnel in the existing old-brick tunnel, two innovative systems were used: displacement measurements by digital camera imaging (cf. § 3.3) and DFOS (Alhaddad et al., 2014). The DFOS measurements using BOTDR allowed to identify localized high strains in the masonry and to detect the associated cracking.

Two examples of tunnel lining monitoring with DFOS to measure the strains arising during construction, using BOTDR, and check the design assumptions are also given by Kechavarzi et al. (2016): the National Grid London Power Tunnel, where DFOS were embedded in the pre-cast SFR concrete lining segments, and a SCL tunnel for Crossrail Liverpool Street station. In the latter, DFOS were embedded to monitor the strain change in the lining in correspondence of the opening of a cross-passage (breakout and excavation).

It is also worth mentioning the long-term structural health monitoring of an existing concrete-lined tunnel facility at CERN (Geneva; Switzerland), where Brillouin optical time domain analysis (BOTDA) allowed detecting strain changes that did not exceed $20 \mu\epsilon$ (Di Murro et al., 2016).

The application of DFOS to measure tunnelling induced ground horizontal strains and displacements has been tested in field trials by Klar et al. (2014), that deployed a shallow fibre optic sensing cable (0.5 m deep) at two sites: during the TBM excavation of a 3 m-diameter, 18 m-deep tunnel, and for pipe-jacking a 1 m-diameter, 6 m-deep water main. Measurements were taken using two different optical technologies, the Brillouin OTDA (with accuracy of $5 \mu\epsilon$) and the back scattered Rayleigh reflectometry (with accuracy $<1 \mu\epsilon$). The fiber optic readings allowed accurate measurements, providing information about volume loss, trough width (position of the inflection point) and ratio between trough length and width. The comparison between the measurements obtained by the two different technologies demonstrated an excellent agreement, although the Rayleigh reflectometry would be a better candidate to obtain the trough length, thanks to its higher spatial resolution. An investigation at laboratory scale on the performance of Rayleigh reflectometry to monitor soil horizontal strain induced by deep underground movements – involving comparison with Particle Image Velocimetry and numerical Finite Element back-analysis – has been recently carried out by Della Ragione et al. (2023a).

3.2 Differential SAR interferometry

Interferometric Synthetic Aperture Radar (InSAR) uses the phase difference between two high-resolution radar images to extract information about topography

within a specific area. A Synthetic Aperture Radar (SAR) is a side-looking imaging radar system that exploits the Doppler effect (i.e. the change of frequency wave perceived by an observer moving relative to the source of the wave) due to the motion of the receiving antenna, to synthesize a much larger aperture. This improves the azimuth resolution, otherwise limited by the ratio between the antenna size and the range, or distance to the target (r_0 in Figure 6). Airborne and spaceborne (satellite) SAR systems allow retrieving a large amount of information on the Earth's topography. As mentioned in § 2, Differential InSAR (DInSAR) can be used to detect the displacement occurring between two subsequent images. However, to discriminate from measurement the effect of atmospheric changes in the same time interval, suitable procedures are required. Since the early 2000's, many techniques have been proposed.

In this framework, Persistent Scatterers Interferometry (PSI) aims at identifying targets on the Earth surface that have a stable phase in time (persistent). These targets (PS) are characterized by high reflectivity and often correspond to point-wise scatterers.

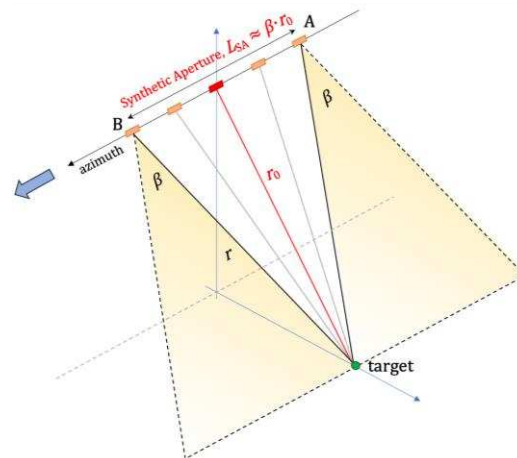


Figure 6. SAR schematic (modified after Meyer, 2019).

The first PSI technique is the pioneering Permanent Scatterers approach (PSInSAR®) proposed by Ferretti et al. (2000, 2001), later extended to include in the analysis less bright Distributed Scatterers (Ferretti et al., 2011). The Small Baseline Subset (SBAS) technique (Berardino et al., 2002), developed immediately after PSInSAR®, is one of the most extensively used. Several other PSI techniques have been developed, as Hooper et al. (2004) or Perissin and Wang (2012): a careful review is provided by Crosetto et al. (2016). Since brighter pixels are characterized by high signal-to-noise ratio, all the mentioned methods achieve improved measurement accuracy.

Once targets are selected, their movement along the sensor-to-target direction (or Line of Sight, LoS) can be detected from the phase variation between two SAR acquisitions. This requires that an accurate Digital Elevation Model is available, and the corresponding phase variation removed, that the geometrical decorrelation, resulting from two distinct viewing geometries is purged, and that the so-called residual topographic error (the difference between the true elevation of the PS centre and that resulting from DEM) is accounted for. Finally, several algorithms have been proposed to estimate and filter out from the interferograms the atmospheric phase component (e.g., Zebker et al., 1997; Ding et al. 2008; Perissin et al. 2011).

The lack or low density of Permanent Scatterers, occurring mostly in non-urban areas, can be partially addressed by using X-band (frequency from 8 to 12 GHz, wavelength, $\lambda = 25$ to 37.5 mm) very high-resolution SAR data — e.g. from TerraSAR-X or COSMO-SkyMed constellations— in comparison to C-band (4 to 8 GHz, 37.5 to 75 mm) — e.g. from Envisat or Sentinel constellations. In addition, artificial Corner Reflectors (CRs) can be deployed on site, that result in good interferometric phases to derive the displacement with higher accuracy. Under optimal conditions (high quality PSs and minimum atmospheric effects) sub-millimetre accuracy was obtained in PSInSAR time series (Ferretti et al. 2007).

However, two limitations of DInSAR and PSI must be mentioned: the one-dimensional nature of measurements (along the LoS) and the “*wrapped phase*” ambiguity. The former implies that only one component of the target displacement is directly measured: its projection into the LoS direction. When ascending and descending SAR data are available, they can be independently processed to calculate vertical and East-to-West horizontal components, hence partially addressing the issue. Different methods have been proposed to derive 3D deformation from DInSAR (Hu et al, 2014), either by combining different datasets, or by making use of auxiliary GNSS, or by making assumptions, the latter being the most widely adopted. On the other hand, wrapped phase limits the ability of PSI to measure “fast” (compared to the satellite revisit time) or, equivalently, “large” displacements. When the differential displacement over the revisit time is larger than $\lambda/4$ – corresponding to the limit “wrapping” value of phase, π – the phase information would be affected by phase

cycle loss, hence the actual displacement would be underestimated and difficult to be retrieved unambiguously. Despite several research efforts this issue does not seem completely solved. Wu et al. (2022) have recently proposed a method for phase unwrapping suitable for displacement monitoring in urban areas.

A review of the use of InSAR to displacement monitoring in geotechnical engineering has been carried out by Shimizu (2022). A few applications to monitor tunnelling induced displacements have been carried out in the last decade. Barla et al. (2016) performed a multi temporal-InSAR analysis on Cosmo SkyMed SAR images in both the ascending and descending direction. The measured displacements agree well with the conventional survey (robotic total station and GNSS). In urban area, a series of works dealing with the use of InSAR data in post-tunnelling damage assessment procedures were carried out by Milillo et al. (2018), Giardina et al. (2019) and Macchiarulo et al. (2021). These papers focus on the construction of Crossrail tunnels in London (UK) showing how multi-temporal InSAR was used to assess the extent of damage to over 800 affected buildings. Applications in the urban area of Naples (Italy) have been carried out by Santangelo et al. (2021) and Della Ragione et al. (2023), the latter aimed to get a “remote” assessment of volume loss.

Recently, Di Mariano et al. (2024) have compared the ground movements measured with conventional optical survey nearby Foneria station during tunnel construction for a branch of metro Line 9 (now Line 10 South) in the city of Barcelona (Spain) with those measured by PSInSAR® analyses of TerraSAR-X images. Figure 7 shows a comparison between the two data sets in transverse section, in approximately greenfield conditions. A large scatter can be seen in the PSInSAR® measured settlement that were fitted by a Gaussian curve. Nevertheless, fitting curves corresponding to the conventional monitoring (highly correlated) and to the InSAR monitoring are very close to one another and result in similar values of volume loss and inflection point distance. In the same figure a comparison between the InSAR profile of the tunnelling-induced settlement of a monitored building block and the corresponding readings from the total station survey indicates that both trend and magnitude are very close. In fact, the higher “visibility” of PSs on the building roof likely improved the quality of the backscattered radar signal, hence the measurements.

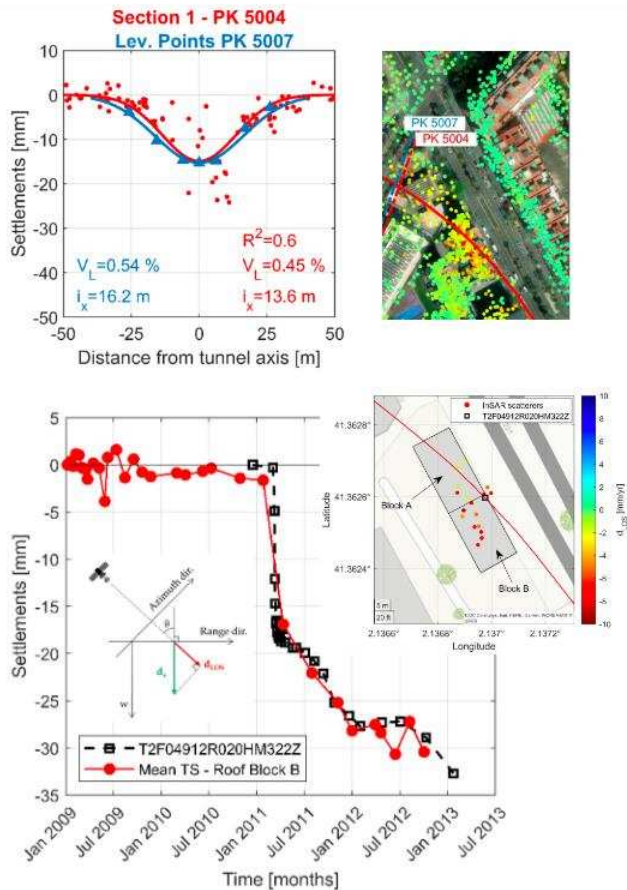


Figure 7. Barcelona Metro Line 10: comparison between conventional monitoring and PSInSAR® (modified after Della Ragione, 2024; Di Mariano et al., 2024).

This allowed to validate PSInSAR® monitoring, showing how it can be used after tunnel construction to expand the existing dataset from conventional survey and to control reliably the evolution of displacements in the long-term.

Serrano-Juan et al. (2016, 2017) carried out an application of both satellite and ground-based InSAR (GB-SAR, or Terrestrial In-SAR) in a construction site affected by underground works in Barcelona, in addition to conventional levelling, highlighting that besides accurate displacement measurements, the GB-SAR automation allows for high-density temporal coverage and concluding that the combined use of different techniques may result in a deeper understanding of the impact of subsidence on nearby buildings. A review of GB-InSAR for deformation monitoring is made by Monserrat et al. (2014).

3.3 From range sensing to range imaging sensing

As mentioned in § 2, among range sensing techniques, high-precision terrestrial laser scanning (TLS) can capture spatial coordinates of a target with sub-millimetric accuracy. Typically, several laser beams are used to scan the objects, producing a point cloud

that is used to construct a detailed model. This technique is suitable to measure ground and structure deformation in contactless mode and in a wide range of environmental conditions, including low-light underground excavations. Deformation monitoring is carried out using change detection methods to track the target position or shape change at different epochs. Different detection methods can be adopted: point-to-point, line-to-line and surface-to-surface: an exhaustive review has been done by Shen et al. (2023).

The current practice for engineering applications focuses mainly on point-based methods since they generally achieve the required accuracy. In the framework of monitoring, these methods need to consider that since distinct scans cannot be identical, it is not possible to sample the same point in two different acquisitions. Therefore a “deformation monitoring block” should be identified and used for tracking. The *Fitting method* and the *Geometric Centre method* are suitable to carry out coordinate calculations of the target thus identified, the former often involving regular shape targets (even artificial), the latter suitable to process more irregular shapes. Alternatively, *Cloud-to-Cloud comparison* (C2C, Girardeau-Montaut et al., 2005) can be carried out. The simplest application of C2C is the *Nearest Point method*, that finds the closest corresponding points in clouds from two subsequent epochs and assumes their distance as relative displacement. If a model surface can be interpolated among the cloud points, the method evolves in a *Cloud-to-Model method* (C2M), where the detection of displacement is based on the distance between cloud points and the reference model surface, along the normal direction to the surface. A further evolution is the *Multiscale Model-to-Model Cloud Comparison*, M3C2 (Lague et al, 2013). The large amounts of data that is produced by point-based approaches can be overcome by feature-based approaches, that involve line or surface fittings on the features extracted from the point-cloud. However, within the framework of terrestrial laser scanning there is still a need for further research about line-based and surface-based deformation monitoring (Shen et al., 2023). In tunnel monitoring, TLS has been generally applied for deformation monitoring during the operational phase, in terms of profile and section deformation, clearance inspection and crack detection.

For the case of St. Mary Abchurch described above (Acikgoz et al. 2022, Pascariello et al. 2023a, b), TLS was successfully employed to monitor displacements of the building façades. Changes in the bottom elevation of the parapet wall were detected using the Piecewise Alignment Method, PAM (Teza et al., 2007) and M3C2 (Lague et al., 2013). The point clouds (Figure 8) were post-processed to determine the

tunnelling-induced displacements. The figure presents a comparison between a near-continuous profile of vertical displacements along the South façade, calculated using the PAM method from changes between the point cloud obtained on March 23rd, 2017 (before tunnelling) and January 16th, 2018 (after the tunnel face completely passed the building) and the corresponding socket displacements.

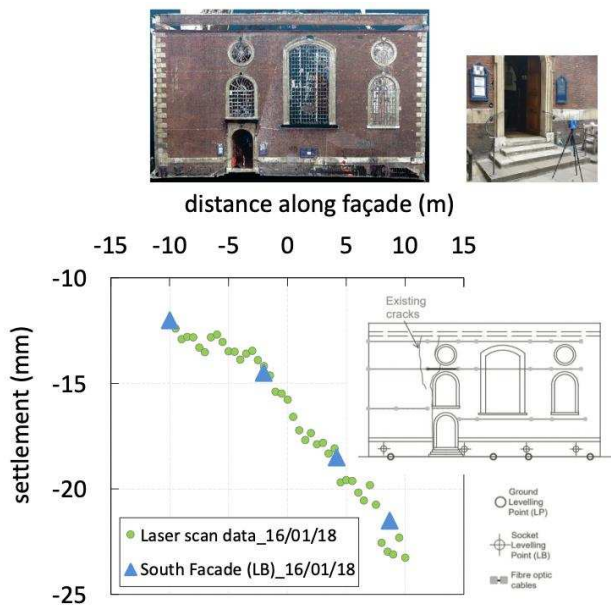


Figure 8. Monitoring St Mary Abchurch during BSCU: South façade point cloud; TLS derived displacements compared to socket settlements (Pascariello et al., 2023a, b).

The agreement between the two data sets is very good. However, the laser scan continuous profile additionally reveals a change of gradient above the doorway, corresponding to the pre-existing crack. Therefore, the profile obtained from levelling is not due to a gradual façade hogging but produced by a local relative rotation between the two edges of the pre-existing crack. This confirmed the measurements of FBG sensors (see Figure 5), indicating that the crack further opened during tunnel construction.

Nowadays, digital photography has reached a technological level that it can potentially replace more traditional and expensive surveying technologies (Soga and Schooling, 2016). Similarly to LiDAR scanners, time-of-flight (ToF) cameras can be employed for ranging, where the entire “scene” is captured with a single light pulse, rather than point-by-point with a rotating laser beam (as in LiDAR scanners). This class of imaging techniques, able to measure the distance of points as a function of time travel of a particular wave emitted from the sensor and bounced back from an object surface, allows to perform a so called “range imaging sensing”.

Advances in digital imaging quality enable the use of different types of sensors for non-contact range sensing that can create 3D point clouds based on multiple overlapping of 2D images (Soga et al., 2019). Lighting is of course a crucial issue to be carefully addressed. In proper light conditions, even consumer-grade digital cameras can be successfully used to produce a point cloud by taking multiple overlapping 2D images of a scene and applying photogrammetry or by employing Structure-from-Motion (SfM) technique to extract a 3D model from a series of images taken from different viewpoints (Schonberger and Frahm, 2016). A system which can detect visual changes on concrete tunnel linings, such as cracks and leakage, has been recently developed by Stent et al. (2016).

Photogrammetry involves processing images to obtain geometric and physical information about the photographed objects: details on its industrial applications can be found in Luhmann (2010). In civil engineering, both aerial and close-range image capturing are carried out for monitoring purpose. However, in underground engineering, the former is less usual due to the complex construction environment, although it is receiving increasing interest. Close-range photogrammetry and DIC (Digital Image Correlation) or PIV (Particle Image Velocimetry; Stanier et al., 2016) have received more attention in the last fifteen years for the periodical inspection of existing tunnels (Attard et al., 2018).

An interesting application of close-range photogrammetry to monitor the structural displacements induced by tunnelling is reported by Alhaddad et al. (2018) for a case study at Moorgate station in London, as part of the construction of the Elizabeth line. A new connection tunnel was built to link the new station to the existing platform tunnels. This required a new stair adit tunnel (5.2 m wide SCL inclined tunnel with varying heights) to be constructed upwards, directly beneath an existing escalator tunnel (D = 4.3 m, cast-iron segmental lining). Tight limits to the escalator deformation were set, hence continuous monitoring was needed during construction. Three digital single lens reflex cameras (with 55 mm focal length) were installed to monitor three separate spaces of the escalator, in addition to conventional monitoring with total stations. The cameras were set to take images every 5 minutes. Up to 18 targets were installed in each monitored section of the escalator tunnel. Each camera was equipped with a tiltmeter, allowing monitoring target settlements relative to the camera, and a retro target, needed for a direct comparison with less frequent total station measurements. This comparison showed a good match between photogrammetry and total station monitored settlements (Figure 9). The Authors showed that with

photogrammetric monitoring a sub-millimetric accuracy of measurements can be reached, compared to millimetric accuracy of automatic total stations, at a much lower cost of the equipment. Moreover, the DIC system's high precision (i.e. random difference between multiple measurements of an unchanged value) enabled measuring the escalator curvatures over very short chords, that are highly sensitive to noise.

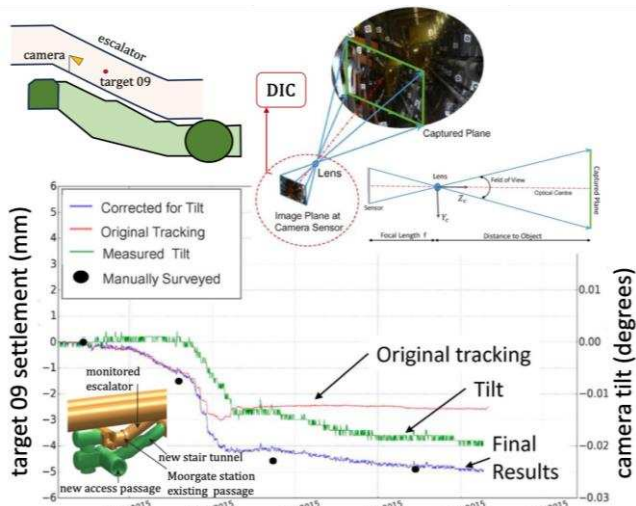


Figure 9. DIC system compared to total station results at Moorgate station (modified after Alhaddad et al. 2018).

Recently, Dalgic et al. (2023) described an experimental campaign aimed at measuring the response of two-storey masonry buildings to foundation settlement profiles mimicking those induced by tunnelling. In the experiments, synchronized video cameras and 2D DIC were used as the primary measurement system for crack detection and to estimate the crack size and length. The photogrammetry was complemented by secondary measurement systems consisting of displacement transducers (LVDTs) and FBG fibre-optic strain gauges to capture the deformed shapes of the structures. The comparative analysis of the collected data sets demonstrated their consistency.

3.4 Wireless Sensor Network (WSN)

On-site cables connecting sensors in large construction sites can be difficult to handle and to protect from possible damages, due to the extensive works that characterise those sites. For this reason, wireless technology has been increasingly applied in tunnel projects in the last decades to avoid deploying too many transmission cables. For instance, Bilotta & Russo (2013) used wireless data loggers to gather frequency measurements from vibrating wire strain gauges embedded in precast reinforced concrete segments for tunnel lining, thus monitoring their

structural behaviour throughout the entire life cycle: from the production phase, during installation and in the long term. Since then, technological improvements permitted to reduce the size of the sensors and their power consumption while the development of new communication protocols allowed larger distance to be covered. Many “established” sensors listed in Table 1 have been innovated in recent years to improve their resolution, to reduce power consumption and to enable them to be integrated in a network, thanks to wireless communication. Micro-electromechanical system (MEMS) sensors combine mechanical and electronic modules, allowing for both sensing and data processing and transmission in a very small space. Due to their high resolution, low power consumption, easy deployment in large number, and high potential for integration in a wireless network, they have been increasingly applied during underground construction in the last years, as pilot Wireless Sensor Networks (Soga and Schooling, 2016). However, expert knowledge is needed to reliably set up the wireless network environment and the interoperability of different WSN is very limited. Therefore, their use in construction projects remains limited, primarily by the contractors' perception of a lower reliability compared to a wired system, that is not compensated enough in terms of structural safety by the MEMS high sensing accuracy (Ma et al., 2021). To boost their acceptance, guidelines for the application of WSN to civil infrastructures have been developed by the Cambridge Centre for Smart Infrastructure and Construction (Rodenas-Herráiz et al., 2016).

4 CONCLUSIONS

The main features of both established and emerging technologies to monitor tunnelling-induced displacements and strains have been discussed in the paper. Future trends for structural health monitoring during tunnel construction should be identified in the perspective of an ideal extension of the use of sensors to monitor the performance of structures in their whole life cycle. This includes not only the construction process, but also the use, service, and dismantling of structures.

The increasing use of the emerging sensing technologies presented in the paper (Fibre-optic sensors, InSAR based techniques, imaging and photogrammetry, WSN) to monitor the effects on existing structures and infrastructures of adjacent tunnelling and underground construction can provide evidence of their ability to secure high safety levels, thus making the way to life-cycle structural “performance” monitoring. However, potential

obstacles to their wider adoption should be overcome. For instance, optical fibres take time to install, which may discourage their use, also in view of their mechanical vulnerability. Therefore, a technological breakthrough is needed to make fibre-optic sensors more robust and easier to install. On the other hand, the use of photogrammetry and range imaging will advance more through improved lighting (which is a major problem in underground environment) than through upgraded equipment.

Monitoring technologies will also be enhanced by advances in algorithms. It is the case of PS-InSAR: PSI algorithms should be improved to reduce the errors due to wrapped phase that affect measurements. Although the current space agency plans to expand the number of SAR missions in the future suggest an increasing use of InSAR monitoring, PSI experts and professionals in charge of interpreting and using PSI results, such as geotechnical engineers, should intensify their collaboration to improve the usability of this technique for monitoring tunnelling-induced displacements on structures.

Overall, the combined adoption of various sensors, as shown in some of the examples in this paper, can better exploit the advantages of each technique, thus helping to capture more accurately both the current state of the structure and its evolution.

Finally, the integration of distributed sensors into wireless systems and the development of increasingly intelligent high-precision micro-sensors (such as MEMS) hint at the possibility of developing machine-learning-based algorithms to increase the accuracy of target identification and of training artificial neural networks to process data sets.

ACKNOWLEDGEMENTS

The Author wishes to acknowledge the collaborative research projects with Cambridge CSIC and UPC-BarcelonaTech that provided some of the results presented in this paper, and the many colleagues that shared their experience on emerging monitoring technologies. He also warmly acknowledges the unvaluable contribution of former and current research students to those projects.

REFERENCES

- Acikgoz, S., Fidler, P.R.A., Pascariello, M.N., Kechavarzi, C., Bilotta, E., DeJong M.J., Mair, R.J. (2021) A Fibre-optic Strain Measurement System to Monitor the Impact of Tunnelling on Nearby Heritage Masonry Buildings, *Int. J. of Architectural Heritage* <http://doi.org/10.1080/15583058.2021.1884318>.
- Acikgoz, S., Luciano, A., Dewhirst, M., DeJong, M.J. Mair, R. (2022) Innovative monitoring of a heritage building during nearby tunnelling in London Clay, *Géotechnique*, <http://doi.org/10.1680/jgeot.19.P.243>.
- Alhaddad, M., Dewhirst, M., Soga, K., Devriendt, M. (2018) A new photogrammetric system for high-precision monitoring of tunnel deformations, *Proc. ICE - Transport*, 172(2), pp. 81-93. Thomas Telford Ltd, <http://doi.org/10.1680/jtran.18.00001>.
- Alhaddad, M., Wilcock, M., Bevan, H., Gue, C., Elshafie, M., Soga, K., Devriendt, M., Waterfall, P., Wright, P. (2014) Multi suite monitoring of an existing cast iron tunnel subjected to tunnelling induced ground movements, *Geo-Shanghai 2014*, China, pp. 357-361.
- Attard, L., Debono, C.J., Valentino, G., Di Castro, M. (2018) Tunnel inspection using photogrammetric techniques and image processing: A review, *ISPRS J. Photogramm. Remote Sens.*, 144, pp. 180–188, <http://doi.org/10.1016/j.isprsjprs.2018.07.010>.
- Barla, G., Tamburini, A., Del Conte, S., Giannico, C. (2016) InSAR monitoring of tunnel induced ground movements, *Geomechanics Tunnelling*, 9(1), pp. 15-22, <http://doi.org/10.1002/geot.201500052>.
- Berardino, P., Fornaro, G., Lanari, R., Sansosti, E. (2002) A new algorithm for surface deformation monitoring based on small baseline differential SAR interferograms, *IEEE TGRS* 40(11), pp. 2375-2383, <http://doi.org/10.1109/TGRS.2002.803792>.
- Bilotta, E., Russo, G. (2013) Internal forces arising in the segmental lining of an earth pressure balance-bored tunnel. *ASCE J Geotechnical and Geoenvironmental Engineering*, 139(10), pp. 1765-1778, [http://doi.org/10.1061/\(ASCE\)GT.1943-5606.0000906](http://doi.org/10.1061/(ASCE)GT.1943-5606.0000906).
- Boje, C., Guerriero, A., Kubicki, S., Rezgui, Y. (2020) Towards a semantic Construction Digital Twin: Directions for future research. *Autom. Constr.* 114, 103179, <https://doi.org/10.1016/j.autcon.2020.103179>.
- Brownjohn J.M.W. (2007) Structural health monitoring of civil infrastructure. *Phil. Trans. Royal Soc. A: Math., Physical and Engineering Sciences*, 365(1851), pp. 589 - 622, <http://doi.org/10.1098/rsta.2006.1925>.
- BTS/ICE (2004). *Tunnel lining design guide*. The British Tunnelling Society and The Institution of Civil Engineers Default Book Series. January 2004, <http://doi.org/10.1680/tldg.29866>.
- Chai, Q., Luo, Y., Ren, J., Zhang, J.Z., Yang, J., Yuan, L., Peng, G.-D. (2019) Review on fiber-optic sensing in health monitoring of power grids, *Opt. Eng.* 58(7), 072007, <http://doi.org/10.1117/1.OE.58.7.072007>.
- Childers, B.A., Froggatt, M.E., Allison, S.G., Moore, T.C., Hare, D.A., Batten, C.F., Jegley, D.C. (2001) Use of 3000 Bragg grating strain sensors distributed on four eight-meter optical fibers during static load tests of a composite structure. In: *Proceedings of the SPIE Conference*, 4332, pp. 133-142, San Diego, CA, <https://doi.org/10.1117/12.429650>.
- Crosetto, M., Monserrat, O., Cuevas-González, M., Devanthy, N., Crippa, B. (2016) Persistent Scatterer In-

- terferometry: A review, *ISPRS Journal of Photogrammetry and Remote Sensing*, 115, pp. 78-89, <http://doi.org/10.1016/j.isprsjprs.2015.10.011>.
- Cumming, I.G., Wong, F.H., (2005) *Digital Processing of Synthetic Aperture Radar Data*, Norwood, MA, Artech House, Inc.
- Dalgic, K.D., Gulen, B., Liu, Y., Acikgoz, S., Burd, H., Marasli, M., Ilki, A. (2023) Masonry buildings subjected to settlements: Half-scale testing, detailed measurements, and insights into behaviour. *Engineering Structures*, 278, art. no. 115233, <http://doi.org/10.1016/j.engstruct.2022.115233>
- Davis, M.A., Kersey, A.D. (1997) Fiber Bragg grating sensors for infrastructure sensing, In: *Proc. Optical Fiber Communication Conference*, Dallas (USA), 177-178, <https://doi.org/10.1109/OFC.1997.719799>.
- Della Ragione, G. (2024) *An integrated approach for assessing the impact of tunnel excavations in urban areas*, PhD Thesis, Univ of Napoli Federico II, Italy.
- Della Ragione, G., Abadie, C.N., Xu, X., da Silva Burke, T.S., Moeller, T., Bilotta, E. (2023a) Fibre optic sensing for strain field measurement in geotechnical laboratory experiments, *Géotechnique Letters* <http://doi.org/10.1680/jgele-2023-048>.
- Della Ragione, G., Rocca, A., Perissin, D., Bilotta, E. (2023b) Volume Loss Assessment with MT-InSAR during Tunnel Construction in the City of Naples (Italy), *Remote Sensing*, 15(10), art. no. 2555, <http://doi.org/10.3390/rs15102555>.
- Di Mariano, A., Gens, A., Della Ragione, G., Bilotta, E., Sanchez, J., Royo, B., Cespa, S. (2024) Case study of soil-structure interaction during tunnelling for Barcelona Metro: a comparison between conventional and innovative displacement measurements, *Proc. 11th Int. Symp. Geotech. Aspects of Underg. Constr. in Soft Ground*, 2024 Macao SAR, China.
- Di Murro, V., Pelecanos, L., Soga, K., Kechavarzi, C., Morton, R. F. (2016) Distributed fibre optic long-term monitoring of concrete-lined tunnel section TT10 at CERN, In: *Proc. International Conference on Smart Infrastructure and Construction*, Cambridge, UK <http://doi.org/10.1680/jfiftsi.61279.027>.
- Ding, X.L., Li, Z.W., Zhu, J.J., Feng, G.C., Long, J.P. (2008) Atmospheric Effects on InSAR Measurements and Their Mitigation, *Sensors*, 8, 5426-5448. <http://doi.org/10.3390/s8095426>.
- Ferretti, A., Fumagalli, A., Novali, F., Prati, C., Rocca, F., Rucci, A., (2011) A new algorithm for processing interferometric data-stacks: SqueeSAR, *IEEE Transactions on Geoscience and Remote Sensing*, 49(9), 3460–3470 <http://doi.org/10.1109/TGRS.2011.2124465>.
- Ferretti, A., Prati, C., Rocca, F. (2000) Nonlinear subsidence rate estimation using permanent scatterers in differential SAR interferometry, *IEEE TGRS*, 38(5), 2202-2212, <http://doi.org/10.1109/36.868878>.
- Ferretti, A., Prati, C., Rocca, F. (2001) Permanent scatterers in SAR interferometry, *IEEE TGRS*, 39(1), 8–20, <http://doi.org/10.1109/36.898661>.
- Ferretti, A., Savio, G., Barzaghi, R., Borghi, A., Musazzi, S., Novali, F., Prati, C., Rocca, F. (2007) Submillimeter accuracy of InSAR time series: experimental validation. *IEEE TGRS*, 45(5), 1142–1153, <http://doi.org/10.1109/TGRS.2007.894440>.
- Floris I., Adam J.M., Calderón P.A., Sales S. (2021) Fiber Optic Shape Sensors: A comprehensive review, *Optics and Lasers in Engineering*, 139, 106508, <http://doi.org/10.1016/j.optlaseng.2020.106508>.
- Giardina, G., Milillo, P., Dejong, M.J., Perissin, D., Milillo, G. (2019) Evaluation of InSAR monitoring data for post-tunnelling settlement damage assessment. *Struct. Control and Health Monit.*, 26(2), e2285.1-19, <https://doi.org/10.1002/stc.2285>.
- Girardeau-Montaut, D., Roux, M., Marc, R., Thibault, G. (2005) Change detection on points cloud data acquired with a ground laser scanner. *International Archives of Photogrammetry, Remote Sensing and Spatial Information Sciences* 36 (Part 3), 30–35.
- González-Arteaga, J., Alonso, J., Moya, M., Merlo, O., Navarro, V., Yustres, A. (2020) Long-term monitoring of the distribution of a building's settlements: Sectorization and study of the underlying factors. *Eng. Struct.* 205, 110111, <http://doi.org/10.1016/j.engstruct.2019.110111>.
- Gue, C.Y., Wilcock, M., Alhaddad, M., Elshafie, M., Soga, K. Mair, R.J. (2015), The monitoring of an existing cast iron tunnel with distributed fibre optic sensing (DFOS), *J. Civ. Struct. Health. Monit.*, (5) pp. 573-586. <https://doi.org/10.1007/s13349-015-0109-8>.
- Güemes, A., Fernández-López, A., Soller, B. (2010) Optical fiber distributed sensing- physical principles and applications, *Structural Health Monitoring* 9(3), pp. 233– 245, <https://doi.org/10.1177/1475921710365263>.
- Hill, K.O., Fujii, Y., Johnson, D.C., Kawasaki, B.S. (1978), Photosensitivity in optical fiber waveguides: Application to reflection filter fabrication, *Appl. Phys. Lett.* 32 (10) 647–649, <https://doi.org/10.1063/1.89881>.
- Hooper, A., Zebker, H., Segall, P., Kampes, B. (2004) A new method for measuring deformation on volcanoes and other natural terrains using InSAR persistent scatterers, *Geophys. Res. Lett.* 31 (23), <https://doi.org/10.1029/2004GL021737>.
- Hoult, N.A., Soga, K. (2014) Sensing solutions for assessing and monitoring tunnels. In: *Woodhead Publishing Series in Electronic and Optical Materials, Sensor Technologies for Civil Infrastructures* (Wang et al.eds), Woodhead Publishing, 56, pp. 309-346, <http://doi.org/10.1533/9781782422433.2.309>.
- Hu, J., Li, Z.W., Ding, X.L., Zhu, J.J., Zhang, L., Sun, Q., (2014) Resolving three-dimensional surface displacements from InSAR measurements: a review, *Earth Sci. Rev.* 133, 1–17. <https://doi.org/10.1016/j.earscirev.2014.02.005>.
- ITA-AITES WG2-Research (2011) *Monitoring and Control in Tunnel Construction*. ITA report n°009.
- Kechavarzi, C., Soga, K., de Battista, N., Pelecanos, L., Elshafie, M., Mair, R.J. (2016) *Distributed Optical Fibre Sensing for Monitoring Civil Infrastructure - A*

- Practical Guide*, ICE Publishing, 192 pp. <http://doi.org/10.1680/dfossmci.60555>.
- Klar, A., Dromy, I., Linker, R. (2014) Monitoring tunneling induced ground displacements using distributed fiber-optic sensing, *Tunnelling and Underground Space Technology*, 40, pp. 141-150, <http://doi.org/10.1016/j.tust.2013.09.011>.
- Lague, D., Brodu, N., Leroux, J. (2013) Accurate 3D comparison of complex topography with terrestrial laser scanner: Application to the Rangitikei canyon (NZ), *ISPRS J. of Phot. Rem. Sens.*, 82, pp. 10-26, <http://doi.org/10.1016/j.isprsjprs.2013.04.009>.
- Luhmann, T. (2010) Close range photogrammetry for industrial applications, *ISPRS J. Photogramm. Remote Sens.* 65 (6), pp. 558–569, <http://doi.org/10.1016/j.isprsjprs.2010.06.003>.
- Ma, E., Lai, J., Wang, L., Wang, L., Xu, S., Li, C., Guo, C. (2021) Review of cutting-edge sensing technologies for urban underground construction, *Measurement*, 167, <https://doi.org/10.1016/j.measurement.2020.108289>.
- Macchiariulo, V., Milillo, P., DeJong, M.J., Gonz ales Mart ı, J., S anchez, J., Giardina, G. (2021) Integrated InSAR monitoring and structural assessment of tunnelling-induced building deformations, *Structural Control and Health Monitoring*, 28(9), e2781, <http://doi.org/10.1002/stc.2781>.
- Mair, R.J. (2008) Tunnelling and geotechnics: New horizons. *Geotechnique*, 58 (9), pp. 695-736
- Meltz, G., Morey, W. W., Glenn, W. H. (1989) Formation of Bragg gratings in optical fibers by a transverse holographic method, *Opt. Lett.* 14, pp. 823-825, <https://doi.org/10.1364/OL.14.000823>.
- Meyer, C., Cucino, P., Eccher, G., Ulrich, D. (2013) The Florence high-speed railway hub: 4D monitoring - Innovations in data acquisition and data management for tunnelling projects in sensitive urban areas. In: *Proc. of WTC 2013*, Geneva (Switzerland), pp. 1403–1410.
- Meyer, F. (2019) Spaceborne Synthetic Aperture Radar – Principles, Data Access, and Basic Processing Techniques, In: *SAR Handbook: Comprehensive Methodologies for Forest Monitoring and Biomass Estimation* (Flores et al. eds). NASA. <http://doi.org/10.25966/ez4f-mg98>.
- Meyer, T.H., Roman, D.R., Zilkoski, D.B. (2005) What does height really mean? Part IV: GPS Heighting. *Surv. & Land Information Science*, 66(3), pp. 165-183, https://opencommons.uconn.edu/nrme_articles/5.
- Milillo, P., Giardina, G., DeJong, M.J., Perissin, D., Milillo, G. (2018) Multi-Temporal InSAR Structural Damage Assessment: The London Crossrail Case Study, *Remote Sens.*, 10(2), 287, <http://doi.org/10.3390/rs10020287>.
- Mohamad, H., Bennet, P.J., Soga, K., Mair, R.J., Bowers, K. (2010) Behaviour of an old masonry tunnel due to tunnelling-induced ground settlement. *G otechnique* 60(12): 927-938, <https://doi.org/10.1680/geot.8.P.074>.
- Mohamad, H., Soga, K., Bennet, P.J., Mair, R.J., Lim, C.S. (2012) Monitoring twin tunnel interaction using distributed optical fiber strain measurements. *ASCE J. Geotech. Geoenv. Engineering*, 138(8), pp. 957-967, [https://doi.org/10.1061/\(ASCE\)GT.1943-5606.0000656](https://doi.org/10.1061/(ASCE)GT.1943-5606.0000656).
- Monserrat, O., Crosetto, M., Luzi, G. (2014) A review of ground-based SAR interferometry for deformation measurement, *ISPRS Journal of Photogrammetry and Remote Sensing*, 93, pp. 40-48, <http://doi.org/10.1016/j.isprsjprs.2014.04.001>.
- Morino A., Balestrieri A., Carrieri G., Martino M., Pezzetti G. (2023) Monitoring. In: *Handbook on Tunnels and Underground Works* (Bilotta E. et al. eds.), 2 (5), SIG - Societ  Italiana Gallerie, CRC Press.
- Moss, R. M., Matthews, S. L. (1995) In-service structural monitoring—a state of the art review, *Struct. Eng.* 73, 23–31.
- N other, N. (2010) *Distributed Fiber Sensors in River Embankments: Advancing and Implementing the Brillouin Optical Frequency Domain Analysis*, PhD Thesis, Technical University of Berlin (Germany).
- Odolinski, R., Teunissen, P.J. (2020) Best integer equivariant estimation: Performance analysis using real data collected by low-cost, single-and dual-frequency, multi-GNSS receivers for short-to long-baseline RTK positioning. *J. Geod.*, 94, pp. 1–17 <https://doi.org/10.1007/s00190-020-01423-2>.
- Pan, Y., Zhang, L. (2021) Roles of artificial intelligence in construction engineering and management: A critical review and future trends, *Autom. Constr.*, 122, 103517, <https://doi.org/10.1016/j.autcon.2020.103517>.
- Pascariello, M.N., Bilotta, E., Acikgoz, S., Schooling J., Mair, R. (2023a) Innovative monitoring and advanced numerical modelling of a heritage masonry building affected by urban tunnelling, *Gallerie e grandi opere sotterranee*, 147, pp. 9-19.
- Pascariello, M.N., Luciano, A., Bilotta, E., Acikgoz, S., Mair, R. (2023b) Numerical modelling of the response of two heritage masonry buildings to nearby tunnelling. *Tunnelling and Underground Space Technology*, 131, art. no. 104845, <http://doi.org/10.1016/j.tust.2022.104845>.
- Perissin, D., Wang, T., (2012) Repeat-pass SAR interferometry with partially coherent targets, *IEEE TGRS*, 50 (1), 271–280. <http://doi.org/10.1109/TGRS.2011.2160644>.
- Perissin, D., Wang, Z., Wang, T. (2011) The SARPROZ InSAR tool for urban subsidence/manmade structure stability monitoring in China. In: *Proc. 34th Int. Symp. Remote Sensing of the Environment (ISRSE)*, Sydney (Australia).
- Qu, X., Shu, B., Ding, X., Lu, Y., Li, G., Wang, L. (2022) Experimental Study of Accuracy of High-Rate GNSS in Context of Structural Health Monitoring, *Rem. Sens.* 14(19), 4989, <https://doi.org/10.3390/rs14194989>.
- Rodenas-Herr aiz, D., Soga, K., Fidler, P., de Battista, N. (2016) *Wireless sensor networks for civil infrastructure monitoring—a best practice guide*, ICE Publishing, London, UK.
- Santangelo, V., Bilotta, E., Di Martire, D., Ramondini, M., Russo, G. (2021) An application of A-DInSAR for monitoring tunnelling-induced displacements in urban area. The case study of the Naples Metro Line 6 stretch

- Mergellina-Chiaia. *Gallerie e grandi opere sotterranee*, 139, pp. 9-16.
- Schonberger, J. L. Frahm, J.-M. (2016) Structure-from-Motion Revisited, In: *Proc. 2016 IEEE Conference on Computer Vision and Pattern Recognition (CVPR)*, pp. 4104–4113, IEEE.
<http://doi.org/10.1109/CVPR.2016.445>.
- Serrano-Juan, A., Pujades, E., Vázquez-Suñè, E., Crosetto, M., Cuevas-González, M. (2017) Leveling vs. InSAR in urban underground construction monitoring: Pros and cons. Case of La Sagrera railway station (Barcelona, Spain), *Engineering Geology*, 218, pp. 1-11,
<http://doi.org/10.1016/j.enggeo.2016.12.016>.
- Serrano-Juan, A., Vázquez-Suñè, E., Monserrat, O., Crosetto, M., Hoffmann, C., Ledesma, A., Criollo, R., Pujades, E., Velasco, V., Garcia-Gil, A., Alcaraz, M. (2016) GB-SAR interferometry displacement measurements during dewatering in construction works. Case of La Sagrera railway station in Barcelona, Spain, *Eng. Geol.*, 205, pp. 104 - 115,
<http://doi.org/10.1016/j.enggeo.2016.02.014>.
- Shen, N., Wang, B., Ma, H., Zhao, X., Zhou, Y., Zhang, Zh., Xu, J. (2023) A review of terrestrial laser scanning (TLS)-based technologies for deformation monitoring in engineering, *Measurement*, 223, 113684,
<http://doi.org/10.1016/j.measurement.2023.113684>.
- Shimizu, N. (2022) Application of satellite technology (GPS and SAR) for monitoring ground surface displacements in rock and geotechnical engineering, In: *Proc. 20th ICSMGE– Rahman and Jaksa (Eds)*. AGS, Sydney, Australia, pp. 597-616.
- Soga, K. (2014) Understanding the real performance of geotechnical structures using an innovative fibre optic distributed strain measurement technology. *Rivista Italiana di Geotecnica*, 4, 7-48.
https://associazionegeotecnica.it/wp-content/uploads/2017/05/rig_4_2014_soga-.pdf.
- Soga, K., Schooling, J. (2016) Infrastructure sensing, *Interface Focus* 6, 20160023,
<http://doi.org/10.1098/rsfs.2016.0023>.
- Soga, K., Luo, L. (2018) Distributed fiber optics sensors for civil engineering infrastructure sensing, *J. Struct. Integrity and Maintenance*, 3(1), pp. 1-21,
<http://doi.org/10.1080/24705314.2018.1426138>.
- Soga, K., Ewais, A., Fern, J., Park, J. (2019) Advances in Geotechnical Sensors and Monitoring. In: *Geotechnical Fundamentals for Addressing New World Challenges* (Lu & Mitchell eds). Springer Series in Geomechanics and Geoengineering.
http://doi.org/10.1007/978-3-030-06249-1_2.
- Stanier, S.A., Blaber, J., Take, W.A., White, D.J. (2016) Improved image-based deformation measurement for geotechnical applications. *Can. Geotech. J.* 53(5), pp. 727–739,
<https://doi.org/10.1139/cgj-2015-0253>.
- Stent, S., Gherardi, R., Stenger, B., Soga, K., Cipolla, R. (2016) Visual change detection on tunnel linings. *Machine Vision and Applications* 27, 319–330.
<http://doi.org/10.1007/s00138-014-0648-8>.
- Teza, G., Calgaro, A., Zaltron, N., Genevois, R. (2007) Terrestrial laser scanner to detect landslide displacement fields: a new approach. *Int. Journal of Remote Sensing* 28(16), pp. 3425-3446,
<http://doi.org/10.1080/01431160601024234>.
- Vlachopoulos, N. (2023) The use of fiber optics for ground and tunnel support monitoring – Two decades of lessons learned, In: *Proc. WTC 2023*, pp. 2336-2344,
<http://doi.org/10.1201/9781003348030-281>.
- Walton, G., Diederichs, M.S., Weinhardt, K., Delaloye, D., Lato, M.J., Punkkinen, A. (2018) Change detection in drill and blast tunnels from point cloud data, *Int. J. of Rock Mechanics and Mining Sciences*, 105, pp. 172–181, <http://doi.org/10.1016/j.ijrmms.2018.03.004>.
- Wu, S., Zhang, B., Ding, X.L., Shahzad, N., Zhang, L., Lu, Z. (2022) A hybrid method for MT-InSAR phase unwrapping for deformation monitoring in urban areas, *International Journal of Applied Earth Observation and Geoinformation*, 112, 102963,
<http://doi.org/10.1016/j.jag.2022.102963>.
- Zebker, H.A., Rosen, P.A., Hensley, S. (1997) Atmospheric effects in interferometric synthetic aperture radar surface deformation and topographic maps, *J. Geophys. Res. Solid Earth*, 102(B4), pp. 7547–7563,
<https://doi.org/10.1029/96JB03804>.
- Zumberge, J.F., Heflin, M.B., Jefferson, D.C., Watkins, M.M., Webb, F.H. (1997) Precise point positioning for the efficient and robust analysis of GPS data from large networks. *J. of Geoph. Res. Solid Earth*, 102(B3), pp. 5005-5018,
<http://doi.org/10.1029/96JB03860>.

INTERNATIONAL SOCIETY FOR SOIL MECHANICS AND GEOTECHNICAL ENGINEERING



This paper was downloaded from the Online Library of the International Society for Soil Mechanics and Geotechnical Engineering (ISSMGE). The library is available here:

<https://www.issmge.org/publications/online-library>

This is an open-access database that archives thousands of papers published under the Auspices of the ISSMGE and maintained by the Innovation and Development Committee of ISSMGE.

The paper was published in the proceedings of the 18th European Conference on Soil Mechanics and Geotechnical Engineering and was edited by Nuno Guerra. The conference was held from August 26th to August 30th 2024 in Lisbon, Portugal.